Gene 757 (2020) 144929

Contents lists available at ScienceDirect

Gene

journal homepage: www.elsevier.com/locate/gene

Research paper

Sexual reproduction potential implied by functional analysis of SPO11 in *Phaeodactylum tricornutum*

Yufeng Mao[a], Li Guo[a], Yan Luo[a,c], Zhihong Tang[a], Wei Li[b,*], Wen Dong[a,*]

[a] College of Marine Life, Ocean University of China, Qingdao 266003, China
[b] State Key Laboratory of Stem Cell and Reproductive Biology, Institute of Zoology, Chinese Academy of Sciences, Beijing 100101, China
[c] Xishuangbanna Tropical Botanical Garden, Chinese Academy of Sciences. Menglun, Mengla, Yunnan 666303, China

ARTICLE INFO

Keywords:
Functional rescue
Meiotic gene
Phaeodactylum tricornutum
Sexual reproduction
SPO11

ABSTRACT

Phaeodactylum tricornutum is a model microalgae that is widely used to study diatom physiology and ecology. Since the meiotic process and sexual cycle have never been observed directly, *P. tricornutum* has been considered to be an asexual species. However, phylogenetic analysis of the *P. tricornutum* genome has revealed a series of meiosis-specific gene homologues in this species. We identified two copies of differently transcribed SPO11 homologs that contain the conserved motifs of Winged-helix and Toprim domains. The homolog PtSPO11-3 interacts with TopoVIB in yeast two-hybrid analysis, whereas the homolog PtSPO11-2 could rescue the sporulation defect of a Spo11 yeast mutant strain. PtSPO11-2 was also found to be significantly up-regulated at low temperatures in *P. tricornutum* and its key catalytic residue was important to the homolog's function in sporulation. The results herein provide positive clue that meiosis and sexual reproduction could exist in this diatom.

1. Introduction

The presence of sexual reproduction in a species is important for its genetic study, improvement and even modification. The traditional approaches for verifying the sex of an organism are dependent on morphological and cytological methods (e.g. mating, fertilizing behavior and meiotic processes). Accordingly, our knowledge of sexual reproduction is strongly restricted to animals, fungi and some land plants, which represents only a small portion of eukaryotes. Unicellular organisms are the vast majority of eukaryotes, and many abandoned sexual reproduction during evolution, making hybridization, genetic recombination and allele segregation impossible. Our knowledge of the reproduction strategy of unicellular organisms is actually quite limited (Schurko et al., 2009).

For sexual reproduction to occur, meiosis is a genetic exchange process that is absolutely necessary (Malik et al., 2008). A single round of DNA replication takes place followed by two successive divisions, turning the diploid cells to haploid. During meiosis, chromatin is cut to generate double strand breaks (DSB) and is then repaired by homologous recombination to exchange genetic material between sister chromatids (Crismani et al., 2013). Many meiosis-specific genes are also involved in the sequential segregation of homologous chromosomes in the first division and sister chromatids in the second division of meiosis (Bulankova et al., 2010). This molecular machinery behind meiotic recombination is absolutely essential to sexual reproduction for most eukaryotes. The core meiotic recombination machinery exhibits strong conservation between eukaryotes, and machinery components may have first appeared in a common ancestor of animals, plants and fungi (Villeneuve and Hillers, 2001). The proteins that participate in core meiotic recombination are encoded by meiosis-specific genes, which include *SPO11*, *HOP1*, *HOP2*, *MND1*, *DMC1*, *MER3*, *REC8*, *MSH4* and *MSH5* (Malik et al., 2008; Ramesh et al., 2005). Once meiosis is lost, these genes will accumulate deleterious mutations, eventually becoming pseudogenes, non-sense DNA or new genes (Lynch and Conery, 2000; Forche et al., 2008; Hall and Colegrave, 2008), allowing a formerly meiosis-specific gene to be maintained in an asexual lineage (Schurko et al., 2009). The presence of meiosis-specific genes strongly supports the existence of meiosis and sexual reproduction in these species (Dacks and Doolittle, 2001); however, due to neo-functionalization of gene products, their function in sexual reproduction remains

Abbreviations: DAPI, 4,6-diamidino-2-phenylindole; DSBs, double-strand breaks; HWE, Hardy-Weinberg equilibrium; ORF, open reading frame; PI, propidium iodide; RT-PCR, reverse transcription-polymerase chain reaction; RMSD, root mean square deviation; SD, synthetic dropout media; WHD, Winged-helix domain; WT, wild type; YPD, yeast extract/peptone/ dextrose medium

* Corresponding authors at: Institute of Zoology, Chinese Academy of Sciences, 1 Beichen West Road, Chaoyang District, Beijing 100101, China (W. Li). College of Marine Life, Ocean University of China, 5 Yushan Road, Shinan District, Qingdao 266003, China (W. Dong).
E-mail addresses: leways@ioz.ac.cn (W. Li), wdong@ouc.edu.cn (W. Dong).

https://doi.org/10.1016/j.gene.2020.144929
Received 23 December 2019; Received in revised form 19 June 2020; Accepted 27 June 2020
Available online 03 July 2020
0378-1119/

ambiguous in different organisms without direct functional analysis (Schurko et al., 2009).

Phaeodactylum tricornutum Bohlin is a marine pennate diatom that has been studied for decades. Due to its small cellular size and complex morphological changes, the reproductive strategy of this alga is still an enigma in the field. Neither a direct description of sexual reproduction nor a meiosis process have been described for *P. tricornutum*. In fact, clonal population structure, fixed heterozygosity and deviation from the Hardy-Weinberg equilibrium (HWE) have been used as evidence for *P. tricornutum* being classified as an asexual species (De Riso et al., 2009, Falciatore et al., 1999). The genome of *P. tricornutum* has been sequenced (Bowler et al., 2008), and more than 130,000 expressed sequence tags have been collected from cells grown under 16 different conditions (Maheswari et al., 2010). The phylogenetic analysis identified the homologs of five meiosis-specific genes, *SPO11*, *MND1*, *MER3*, *MSH4* and *MSH5* (Patil et al., 2015), which usually play an important role in most eukaryotes. The direct functional analysis of these meiosis-specific genes is critical to obtain a clearer understanding of meiosis and sexual reproduction in this species.

Proper chromosome segregation during the first meiotic division requires pairing of homologous chromosomes mediated by meiotic recombination. DNA DSBs catalyzed by SPO11 are necessary to initiate meiotic recombination and usually for homologous chromosome pairing during meiosis (Carofiglio et al., 2013; Robert et al., 2016b). SPO11 is believed to act as a dimer with the protein interacting in a head to tail pattern to introduce two coordinated active sites (Liu et al., 1995; Robert et al., 2016b). In *Saccharomyces cerevisiae*, SPO11 self-associates in the presence of Rec102 and Rec104, two other meiosis-specific proteins required for DSBs formation (Kee et al., 2004; Sasanuma et al., 2007). In contrast with single homologs in animals and yeast, three homologs are present in *Arabidopsis thaliana* and other higher plants (Jain et al., 2008). In *A. thaliana,* genetic analyses revealed that two SPO11 paralogs (SPO11-1 and SPO11-2) and both of their catalytically active tyrosine residues are required for meiotic recombination. These results suggest a heterologous dimer, consisting of functional SPO11-1 and SPO11-2 proteins, is necessary for meiotic DSBs formation (Stacey et al., 2006; Hartung et al., 2007; Robert et al., 2016b). SPO11-3, ancestral kinship to SPO11 and historical nomenclature in the literature, is a topoisomerase subunit TopoVIA in *Arabidopsis*. TopoVIA/SPO11-3 and TopoVIB of *Arabidopsis* interact and formed the A2B2 heterotetramer of TopoVI (Hartung and Puchta, 2001). TopoVI is thought to serve as the primary topoisomerase for DNA decatenation and supercoil relaxation in archaea and is essential to endoreduplication, cell growth, and mitotic proliferation in plants (Hartung et al., 2002; Yin et al., 2002; Wendorff and Berger, 2018).

In the genome of *P. tricornutum*, phylogenetic analysis found two *SPO11* homologs (Malik et al., 2007; Patil et al., 2015), one at chromosome 10 (chr_10:681001–682299, JGI: 36531) and the other at chromosome 1 (chr_1:1699981–1701563, JGI: 24838). The former was related to the meiotic specific SPO11-2 of plants, whereas the latter was related to SPO11-3 (Patil et al., 2015). Similar to many diatoms, SPO11-1 seems to have been lost in *P. tricornutum* (Sprink and Hartung, 2014; Patil et al., 2015). Whether *P. tricornutum* SPO11 homologs retain their meiotic function is an interesting question. In this paper, we focus on the direct functional analysis of SPO11 homologs in *P. tricornutum*. Structural exploration and functional complementation experiments provide positive signs of meiosis and sexual reproduction in *P. tricornutum*.

2. Materials and methods

2.1. Microalgal culturing

P. tricornutum MACC B228 was obtained from the Key Laboratory of Mariculture of Chinese Ministry of Education, Ocean University of China. The alga was cultured in *f/2* medium (Guillard, 1975) at 22 ± 1 °C and under 24–30 μmol.m^{-2}.s^{-1} irradiation following a rhythm of 12 h light and 12 h dark with occasional shaking (twice a day) and position shifting. On day 6 (exponential phase), the cells were harvested by centrifuging at 4000*g* for 10 min, washed with 1 mL of sterilized seawater, divided into aliquots, and precipitated at 10,000*g* for 2 min. Cell pellets were frozen in liquid nitrogen and stored at −80 °C until processed for genomic DNA or RNA extraction.

In preparation for cell population quantification and gene expression analysis using real-time quantitative PCR, cells were grown for 6 days using the conditions described above. Thereafter, cells were harvested and algae were exposed to low light intensity (4–5 μmol.m^{-2}.s^{-1}), high temperature (28 °C), low temperature (12 °C), ammonium supplemented medium (800 μM NH_4Cl) or resource exhausted seawater (filtered seawater that had been used to culture microalgal more than three months, i.e. resource depleted seawater). Finally, the cells were harvested at different timepoints.

2.2. Multiple sequence alignment and homologs modelling

To find homologs for each gene of interest in *P. tricornutum*, protein sequences from *S. cerevisiae* or *Chlamydomonas* (NCBI) were used as queries in BLASTP searches against the *P. tricornutum* genome at JGI (http://genome.jgi-psf.org/). Deduced amino acid sequences of SPO11 homologs from other species were downloaded from the National Center for Biotechnology Information (NCBI) and used to align the putative amino acid sequences of *P. tricornutum* SPO11 homologies by Multiple Sequence Comparison and Multiple Protein Sequence Alignment (MUSCLE) version 3.8 and BioEditsoftware (Edgar, 2004). NCBI's conserved domain database (Marchler-Bauer et al., 2015) and SMART (http://smart.embl-heidelberg.de) were then applied to identify and annotate domain(s) and region(s) in the protein sequence. Secondary structure prediction was done using the PSIPRED Analysis Workbench (http://bioinf.cs.ucl.ac.uk/psipred/) and colored with ESPript (http://espript.ibcp.fr/). We modeled the tertiary structure of predicted *P. tricornutum* SPO11 proteins using the SWISS-MODEL workspace (Biasini et al., 2014). The closest known structure, type II DNA topoisomerase VI subunit A, was used for modeling homologs. Protein structure comparison was done with FATCAT (http://fatcat.burnham.org/). The structural images were prepared with PyMOL (Schrödinger).

2.3. Expression analysis

Total RNA was extracted from *P. tricornutum* using a Trizol method, following the manufacturer's instructions (OMEGA E.A.N.A. Total RNA Kit II, USA), with any genomic DNA being digested with DNase (TaKaRa). First strand cDNA was generated with a M−MLV RTase cDNA Synthesis Kit (TaKaRa), and second strand cDNA was synthesized with an *E. coli* RNaseH/*E. coli* DNA Ligase Mixture (TaKaRa). Genes of SPO11 homologs were PCR amplified using total *P. tricornutum* cDNA, genomic DNA and DNase-digested genomic DNA (Control) as template. *ACTIN* (JGI:51157) was included as a housekeeping gene. *PtSPO11-3* was detected with primers 5′- GTTTATTTTGCTGGTCGAGAAGG −3′ and 5′- TTAAGTTCCGAGGTGATGCG −3′. Primers used to detect *PtSPO11-2* were 5′- GATTGAGACAGTGGTTTTGGC −3′ and 5′- CGTA AAATGTCGCCTTGCTG −3′. *ACTIN* was amplified using forward primer:5′-ATGTTCCCTGGTATTTCCGAG-3 and reverse primer:5′-TGG AAAGTAGAAAGGGAAGCG-3′. Reverse transcription-polymerase chain reaction (RT-PCR) products were subjected to electrophoresis on a 2% agarose gel. Primers for the amplification of *PtSPO11-3* flank a 75 bp intron. This allows us to distinguish the targeted product from cDNA amplification versus product from amplification of contaminated genomic DNA. Because *PtSPO11-2* and *ACTIN* have no intron, their PCR products are the same size whether amplified from cDNA or genomic DNA.

For gene expression analysis, stationary phase cells were suspended

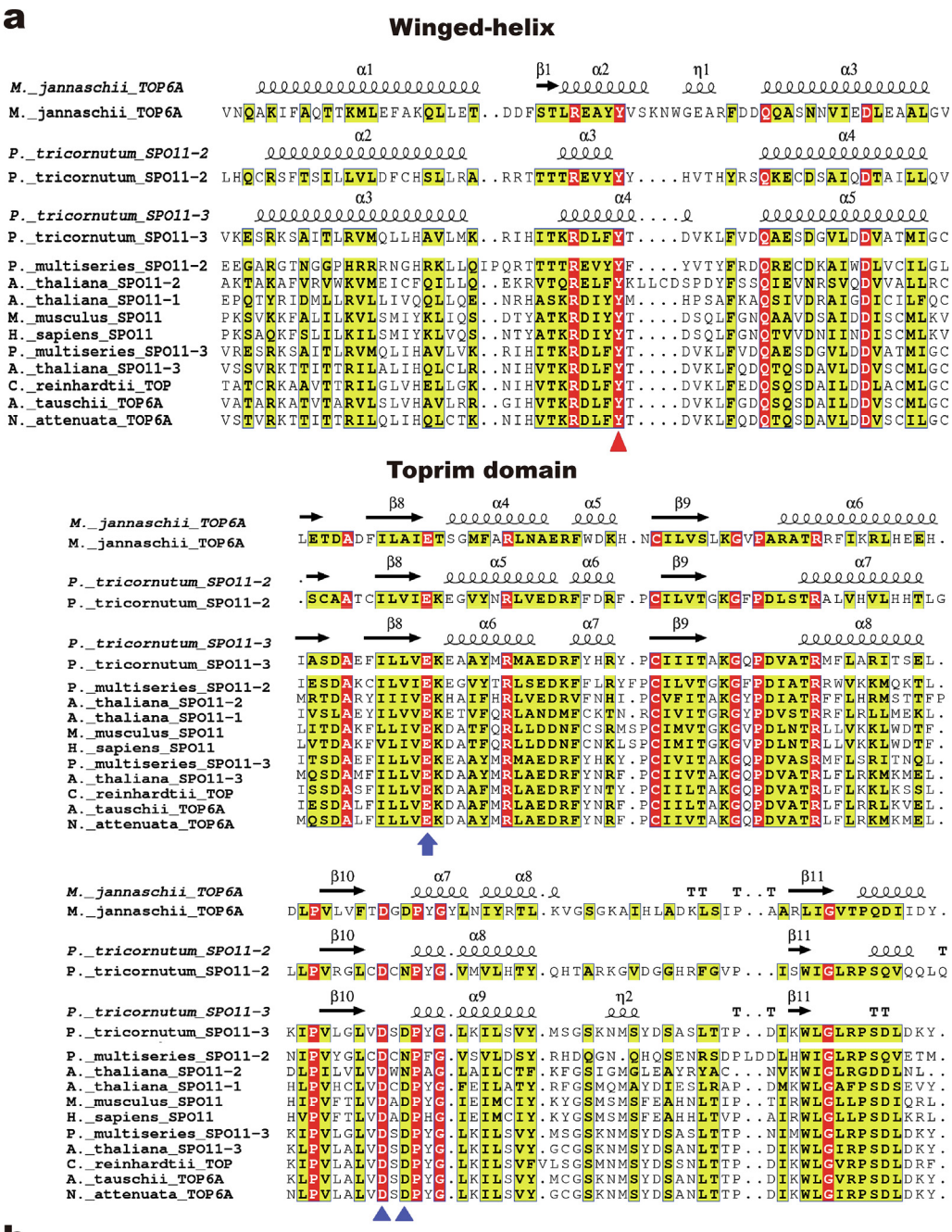

Fig. 1. Multiple sequence alignment and structural comparison of SPO11. a. Multiple alignment of the two modules that are essential for DNA binding and cleavage in SPO11 homologues and *P. tricornutum* SPO11. Winged-helix domain (WHD) and Toprim. The conserved catalytic tyrosine contained in the helix-turn-helix (HTH) motif are indicated by red arrowhead. The cluster of conserved acidic residues (DXD and E) are indicated by blue arrowheads and an arrow. The predicted secondary structure elements are shown above the alignment. b. Comparison of the models of the *P. tricornutum* SPO11 homologs WHD and Toprim domain structures with the *M. jannaschii* TopoVIA structure. WHD is shown in green, and the Toprim domain is shown in magenta (α-helix) and yellow (β-sheet). The catalytic tyrosine and the cluster of conserved acidic residues are emphasized in red and blue correspondingly. Full name of species in Figure: *Methanocaldococcus jannaschii; Phaeodactylum tricornutum; Pseudo-nitzschia multiseries; Arabidopsis thaliana; Mus musculus; Homo sapiens; Chlamydomonas reinhardtii; Asgilops tauschii; Nicotiana attenuate.* (For interpretation of the references to colour in this figure legend, the reader is referred to the web version of this article.)

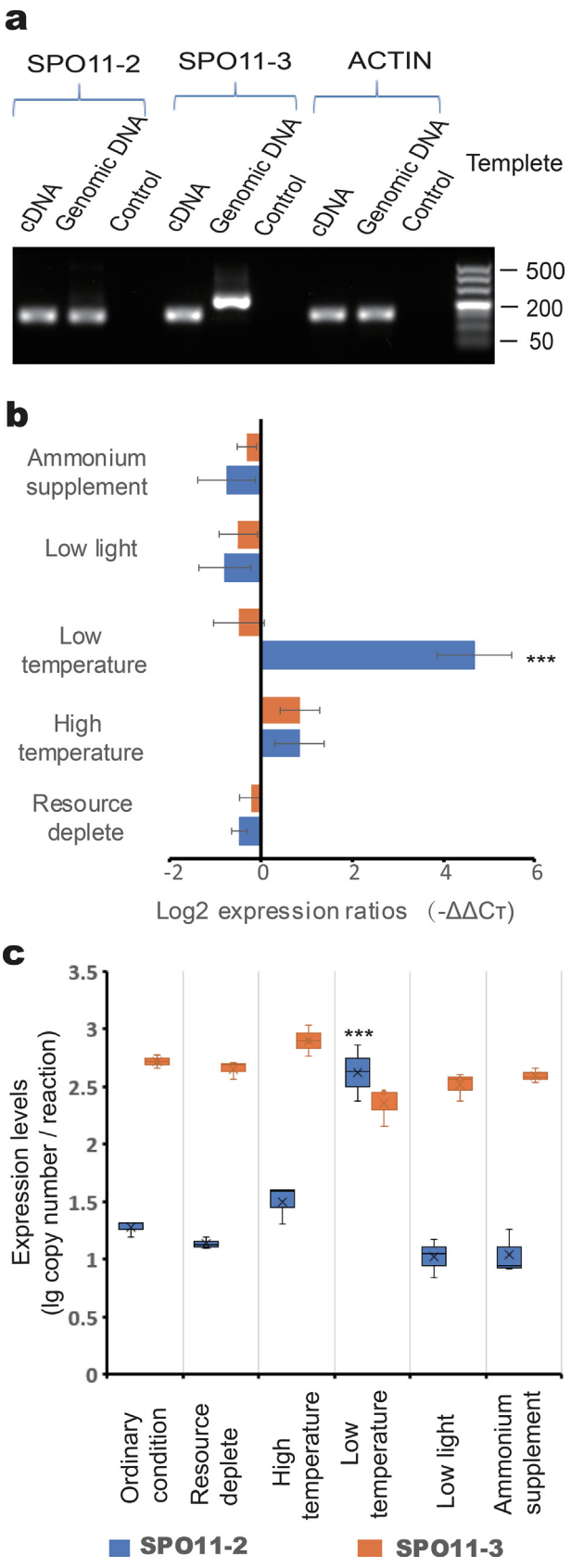

Fig. 2. The PtSPO11-2 and PtSPO11-3 loci were actively transcribed and had different expression patterns. a. Qualitative RT-PCR analysis of *P. tricornutum* SPO11 homolog gene expression. Control: DNase-digested genomic DNA. b. The relative changes of gene transcription among the treatment groups were quantified using the $2^{-\Delta\Delta Ct}$ methods. c. The relative expression levels of the target genes. The number of gene copies per reaction was quantified by standard curve and normalized to that of *ACTIN* gene. ***p < 0.001 vs. untreated cells, paired Student *t* test. Data are shown as mean ± SEM(n = 3).

in new medium and exposed to different conditions for 3 additional days. $1x10^8$–$1x10^9$ cells from triplicate independent cultures were harvested and total RNA was extracted. Real-time quantitative PCR was performed using Applied Biosystems StepOnePlus System (Thermo Fisher Scientific) and SYBR Green PCR reagents (RR047Q, RR420Q, TaKaRa). *ACTIN* was used as a housekeeping gene. The primers for quantitative PCR were the same as those described for RT-PCR. Samples were amplified in triplicate in the presence of 0.5 μM gene-specific primers. A two-step PCR protocol was used. Together, cDNA was denatured at 95 °C for 30 s followed by 40 cycles of denaturing (95 °C for 5 s) plus annealing (60 °C for 30 s). The relative level of gene transcription among the treatment groups was quantified using the $2^{-\Delta\Delta Ct}$ method (Livak and Schmittgen, 2001). PCR-amplified target DNA was diluted in a 10-fold dilution series, from 1 nM to 0.01 pM. Standard curves were derived by linear regression analysis from plot of the CT values of each standard dilution point against the Log of the arbitrary concentration of the DNA dilutions. Amplification efficiency ($E = 10^{-1/slope}$-1) of genes calculated from respective standard curves was: $E_{PtSPO11\text{-}2} = 1.01$, $E_{PtSPO11\text{-}3} = 1.09$, and $E_{ACTIN} = 0.97$. The expression abundances of PtSPO11-2 and *PtSPO11-3* genes were calculated and normalized to that of *ACTIN* gene. Statistical analysis was conducted with SPSS Statistics (IBM, v19.0) and significance evaluated with *t* testing.

2.4. Gene cloning and generation of expression constructs

Candidate genes were cloned from *P. tricornutum* cDNA. The full length SPO11-3 gene was amplified by PCR using a *Bam* HI-inserted sense primer (TAGGATCCATGGCGTCTCGCAACCG) and an *Xba* I-inserted antisense primer (GCTCTAGACTAGATCCAATCTCCTTCC), whereas the full length *PtSPO11-2* gene was amplified using a *Kpn* I-inserted sense primer (TAGGTACCCATGGAGGACCTTATCGAG) and an *Eco* RI-inserted antisense primer (CGGAATTCTCAAATAATATCCATCC AAC). The PCR product and plasmid were digested with the appropriate restriction endonucleases at 37 °C overnight. DNA fragments were purified using a QiaGen DNA Purification Kit and the purified fragment was inserted into *p*YC2/NTC using T4 DNA ligase (TaKaRa). Recombinant plasmids were introduced into *E. coli* Top10 using heat shocking. Recombinants were grown in LB medium supplemented with ampicillin (100 mg/L) at 37 °C. Colony PCR was conducted for primary screening of the recombinants. Recombinant plasmids were isolated and confirmed by restriction analysis. Finally, recombinant plasmids of 5 colonies were sequenced.

2.5. Yeast two-hybrid assays

For the yeast two-hybrid analysis, plasmids pGBT9 and pGAD424 were used to construct bait and activator fusions. The *P. tricornutum* Topo VI B (gi|219125489|) insert was amplified by PCR using an *Eco* RI-linked sense primer (GGAATTCATGGCAAAAACCAACGGCGTG) and a Bam HI-linked antisense primer (CGGGATCCTTATTCTTGAACTTGC ATTGCAGG). The SPO11-3 insert was amplified by PCR using a *Bam* HI-linked sense primer (CGGGATCCGTATGGCGTCTCGCAACCG) and a *Pst* I-linked antisense primer (AACTGCAGCTAGATCCAATCTCCTTCC), whereas the SPO11-2 insert was amplified using an *Eco* RI-linked sense primer (GGAATTCATGGAGGACCTTATCGAG) and a *Pst* I-linked antisense primer (AACTGCAGTCAAATAATATCCATCCAAC). Target DNA fragments were inserted into plasmid vectors and the yeast strain PJ69-4a (trp1-901 leu2-3,112 ura3-52 his3-200 gal4D gal80D LYS2::GAL1-

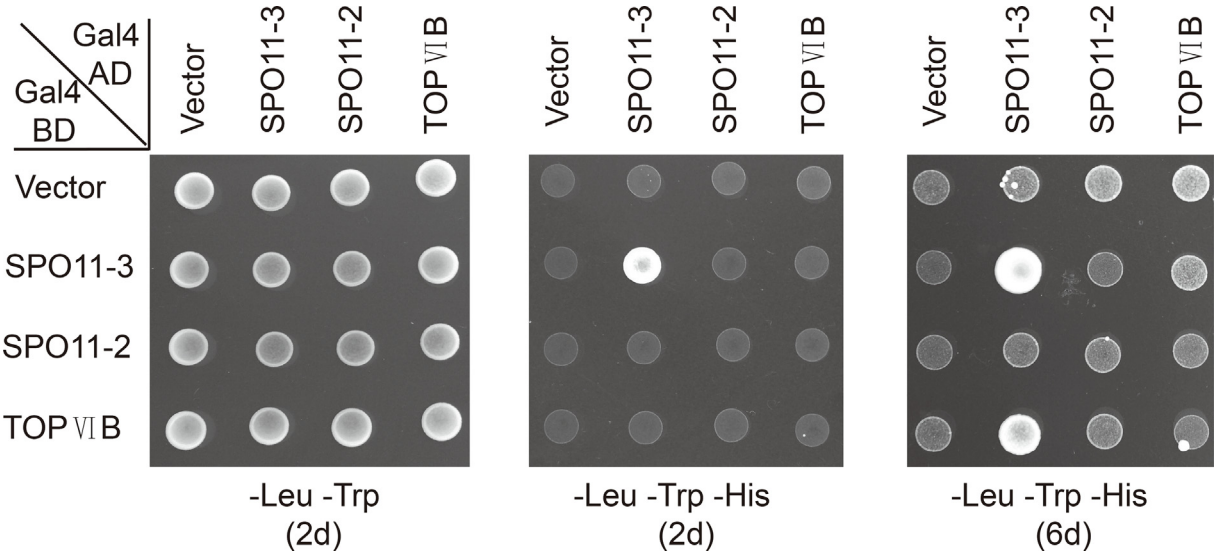

Fig. 3. Yeast two-hybrid analysis of self-association and protein–protein interaction. Growth of PJ69-4A co-transformed with GAL4-BD fused with SPO11-3, SPO11-2 or Topo VI B and GAL4-AD fused with SPO11-3, SPO11-2 or Topo VI B. GAL4-AD and/or GAL4-BD vector were used as negative controls. Photographs were taken after incubation at 28 °C for 2 days or 6 days.

HIS3 GAL2-ADE2 met2::GAL7-lacZ) was co-transformed with bait and prey constructs. Lithium acetate-mediated transformation of yeast strain PJ69-4A was performed as described previously (Gietz and Schiestl, 2007). After transformation, yeast cells were selected with synthetic dropout media (SD) composed of a nitrogen base, 2% glucose and a dropout supplement lacking leucine and tryptophan (-Leu-Trp). The interaction between the two proteins was tested by growing on a histidine-free medium. Cells were grown on SD media lacking leucine and tryptophan or SD medium lacking leucine, tryptophan and histidine (-Leu-Trp-His). 2×10^5 cells were used. Photographs were taken after incubation at 28 °C for 2 days or 6 days.

2.6. Site-specific mutagenesis

A mutant of *SPO11-2* (*SPO11-2 M*) was generated by substituting the TAC codon containing catalytic residue tyrosine(Y) 140 with a TTC codon (F, phenylalanine), using a site-directed mutagenesis method (Chiu et al., 2004). The *P. tricornutum SPO11-2* inserted pYC2/NTC plasmid was amplified by PCR. Mutations were introduced using oligonucleotide pairs (mutation sites were underlined) MUTA-SPO11-2F (TGAAGTTTACTTCTACCACGTGACGCACTACCGCTCCCAAAAAGAATG) and MUTA-SPO11-2R (TCACGTGGTAGAAGTAAACTTCACGGGTTGTTGTTGTACGCCGAGCAC). PCR reactions (50 μL) were set up, containing 1 X KOD plus PCR reaction buffer, 1 mM dNTP (each), 200 μmol primers (forward and reverse), 2 mmol of $MgCl_2$, 1 μL DMSO, 25 ng plasmid, and 1 μL of KOD plus (TOYOBO,1U/μL). PCR was carried out by denaturing at 94 °C for 30 s followed by 32 cycles of denaturing at 55 °C for 30 s plus annealing and extending at 68 °C for 8 min. Next, the PCR product was digested with *Dpn* I (NEB) at 37 °C for 2 h. Finally, 20 μL of digested PCR product was directly used to transform *E.Coli* Top10 cells. Cells were grown in LB medium containing ampicillin (100 mg/L) at 37 °C. The recombinant plasmid was commercially sequenced to verify the mutation. The complementation assay was performed in deletion strains of *S. cerevisiae.*

2.7. Yeast deletion strains

The complementation assay was performed in deletion strains of *S. cerevisiae* in which the target genes were inactivated with a *kanMX* gene (Wach et al., 1994). The deletion cassette was constructed using two sequential PCR reactions. The resulting cassette contained, in the following order, 90 bases directly upstream of the target open reading frame (ORF) (proximal to the start codon), the *kanMX* module, and 90 bases of downstream of the target ORF (distal to the stop codon). The lithium acetate integrative transformation protocol (Gietz and Schiestl, 2007) was used to introduce the gene deletion cassette into diploid yeast cells (BY4743: MAT a/α *his3Δ1/his3Δ1 leu2Δ0/leu2Δ0 lys2Δ0/*LYS2 MET15/*met15Δ0 ura3Δ0/ura3Δ0*) followed by selection of colonies on G418 containing agar plates. The resulting tranformants were sporulated and haploids of both mating types, MAT a and MAT α, were recovered from the tetrads (Brachmann et al., 1998). Strains 941 (BY4741, MAT a, *spo11::kanMX*) and 10,941 (BY4742, MAT α, *spo11::kanMX*) were used. All yeast deletion strains were identified by amplifying *KanMX*.

2.8. Mating and transformation

The diploid mutants of BY4743 (*Lys*$^{\triangle}$; *met*$^{\triangle}$) were obtained from mating single type strains carrying either the *lys2* (BY4742) or *met15* (BY4741) marker and verified using flow cytometry. Briefly, 500 μL of cells were spun down, resuspended in 1 mL 70% ethanol, and spun down again at room temperature for 10 min. The cells were washed with 1 mL of PBS (pH 7.5) and resuspended in 100 μL of PBS (pH 7.5). After adding 2 μL of RNase A (10 mg/mL), the cells were incubated at 30 °C for 2 h, precipitated and stained with propidium iodide (50ug/mL), and analyzed using a BDFACSvantage SE Flow Cytometry System (Franklin Lakes, NJ). The mutant and wild type BY4743 (WT BY4743) strains were transformed with a lithium acetate method (Gietz and Schiestl, 2007).

2.9. Sporulation and statistical analysis

Wild type BY4743, BY4743 carrying *p*YC2/NTC empty vector and BY4743 carrying *PtSPO11-2* and *PtSPO11-3* were first grown to saturation in yeast extract/peptone/ dextrose medium (YPD) for 24 h. They were then washed three times with sterile water and grown again in YPA medium (1% yeast extract, 2% peptone, 1% potassium acetate) supplemented with 0.2% Gal for 24 h. The cells were washed again and resuspended in sporulation medium (1% KAc, 0.2% Gal). Between 0 and 3.5 days, 2 mL cells were harvested at 0.5 day intervals, fixed in 70% ethanol at 4 °C, washed twice in PBS (pH 7.5), and finally stained with 1 μL of 4,6-diamidino-2-phenylindole (DAPI, 50 μg/mL) in the

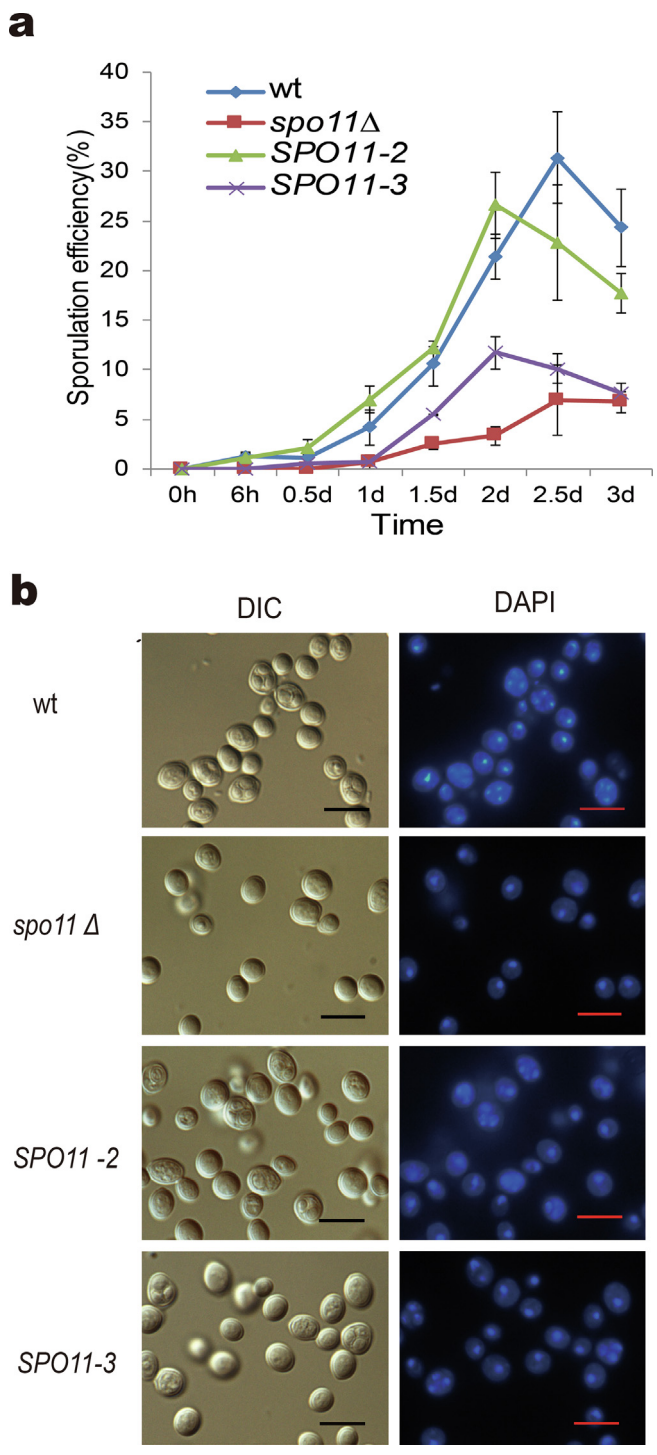

Fig. 4. Complementary approaches and functional assessment of SPO11-2 and SPO11-3 of *P. tricornutum*. a. The sporulation efficiencies of wild type (wt), SPO11 mutant (*spo*11Δ) and two rescue strains (*SPO11-2*, *SPO11-3*). The curves represent the average of three independent experiments and about 200 cells were counted for each timepoint. Data are presented as mean ± SEM. b. Microscope images of wild type (wt), SPO11 mutant (*spo*11Δ) and two other strains (*SPO11-2 SPO11-3*) that had been incubated in sporulation media for 2.5 days, fixed, and then stained with DAPI. Bar = 10 μm.

dark at room temperature for 20 min. Using at least 200 cells, nuclei per cell was counted under a fluorescence microscope. Sporulation was repeatedly observed and sporulation efficiency was calculated and expressed as mean ± SEM (n = 3). Statistical analysis was conducted with SPSS Statistics (IBM, v19.0) and significance evaluated with *t* testing.

3. Results and discussion

SPO11 creates double-strand DNA breaks during the early stages of meiosis and initiates meiotic recombination. These double-strand DNA breaks are repaired by homologous chromosome pairing and recombination. SPO11 homologs are evolutionary conserved and known to be present in almost all sexual eukaryotes, including animals, fungi, plants and some protists (Ramesh et al., 2005; Bloomfield, 2016). Two copies of suspected SPO11 homologous genes in the *P. tricornutum* genome have previously been identified (Patil et al., 2015). Our paper focuses on the structure and meiotic function of those two copies of SPO11 homologous genes and aims to provide information on whether this model diatom has or previously had the ability to undergo sexual reproduction.

3.1. SPO11-2 and SPO11-3 of P. Tricornutum contain Winged-helix and Toprim domains

Winged-helix domain (WHD) and Toprim of SPO11 are essential for DNA binding and subsequent cleavage (Robert et al., 2016b). Deduced amino acid sequences of SPO11 homologs from other species were down loaded from NCBI and used to align putative amino acid sequences of *P. tricornutum* SPO11-2 and SPO11-3 with Multiple Protein Sequence Alignment (MUSCLE). Despite an overall low level of sequence identity and similarity (PtSPO11-2 and PtSPO11-3 share 47% similarity and 29% identity with each other at the amino acid level), key motifs or residues were identified within the WHD and Toprim domains of *P. tricornutum* SPO11-2 and SPO11-3, and the predicted secondary structure was conserved (Fig. 1a). WHD in PtSPO11-2 resided from residues 109 to 164. Tyrosine 140, located within the helix-turn-helix motif, corresponded to the inferred catalytic site that forms a covalent link with DNA during meiotic DSB formation. In SPO11, the Toprim domain resembled a Rossmann-like fold with a central β-sheet formed by four parallel β-strands and flanked by three α-helices. The conserved glutamate (Glu232) was present in the Toprim domain, corresponding to the predicted catalytic site for strand cleavage and rejoining. The importance of this acidic residue has been documented for topoisomerases, and mutations of the conserved glutamate has been shown to completely abolish enzymatic activity (Chen and Wang, 1998). Based on our protein alignments, we predicted the structures of *P. tricornutum* SPO11-2 and SPO11-3 would share strong similarity with that of *Methanocaldococcus jannaschii* TopoVIA (Fig. 1b). Our findings for PtSPO11-2 with 283 equivalent positions and a root mean square deviation (RMSD) of 2.37 and PtSPO11-3 with 287 equivalent positions and an RMSD of 2.59 suggest that the overall organization of the WHD and Toprim domains share structural similarity with *M. jannaschii* TopoVIA. Structural comparison combined with multiple-sequence alignment demonstrated that PtSPO11-2 and PtSPO11-3 were similar to their SPO11 homologs, sharing a highly-conserved DNA binding pattern and spatial conformation.

3.2. The PtSPO11-2 and PtSPO11-3 locus were actively transcribed and had different expression patterns

Transcription is a prerequisite for a functional gene, so we next analyzed whether these two SPO11 homologous genes were expressed or not and to what extent. RT-PCR results indicated that the PtSPO11-2 and PtSPO11-3 locus were all actively transcribed under our culturing condition (Fig. 2a), suggesting these two genes might still be active in this species. This conclusion is also supported by the sequencing and real-time quantitative PCR results.

External environmental factors that induce sexual reproduction are highly variable for different organisms. The environmental factors that trigger formation of sexual cells and sexual reproduction in diatoms are

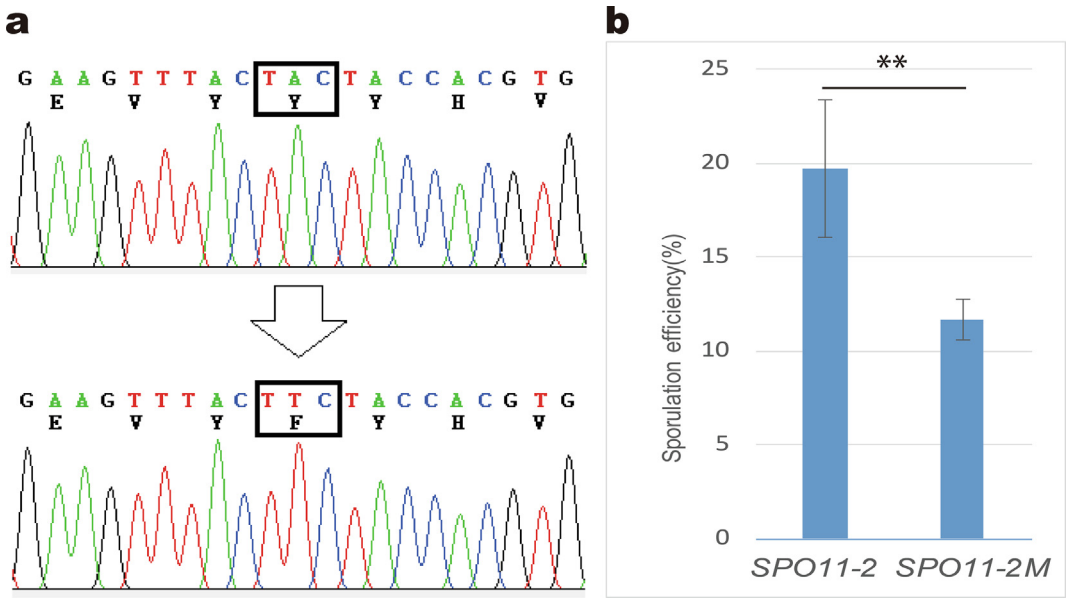

Fig. 5. Y140 of SPO11-2 is important to its function in meiosis. a. The sequencing results for site-specific mutagenesis products, in which the TAC codon for the presumed catalytic residue tyrosine (Y) 140 of *P. Tricornutum* SPO11-2 was successfully substituted by a TTC codon (F, phenylalanine). b. The percentage of mature ascus in SPO11-2 and SPO11-2 M strains after 2.5 days induction for sporulation. Data are presented as mean ± SEM, **p < 0.01 (n = 3).

less well known (Chepurnov et al., Von Dassow and Montresor, 2011, 2010; Moore et al., 2017). In general, sexualization appears to be strongly associated with conditions causing synchronous sexuality in cells experiencing growth stress (Von Dassow and Montresor, 2011; Moore et al., 2017). Thus, by varying stress conditions during culturing, the expression of PtSPO11-2 and PtSPO11-3 were analyzed by real-time quantitative PCR after *P. tricornutum* cells were exposed to low light intensity (4–5 $\mu mol.m^{-2}.s^{-1}$), high temperature (28 °C), low temperature (12 °C) or resource depletion seawater.

The *SPO11-2* gene usually maintains a low level of expression, but it is greatly up-regulated during meiosis in known model organisms. The *SPO11-3* gene is expressed at higher levels, potentially constitutively, in many if not all cells. If the *SPO11-3* gene in *P. tricornutum* has a similar function, it should be expressed at higher levels than SPO11-2. Patil et al. (2015) showed this for the diatom *Thalassiosira weissflogii*, where the SPO11-2 homolog was expressed at lower levels (over three orders of magnitude) than SPO11-3 during asexual conditions and never reached high-level expression, even when a portion of the diatom population was induced to enter meiosis. Our gene expression results suggest a similar situation exists in *P. tricornutum*. Generally, the expression level of PtSPO11-3 was not significantly affected by culture conditions, showing characteristics of constitutive expression (Fig. 2b), and the expression level of PtSPO11-3 was several orders higher than that of PtSPO11-2 (Fig. 2c). It is noteworthy that the expression of PtSPO11-2 significantly increased 3 days after the exponential phase cells incubated at 12 °C, reaching expression levels of PtSPO11-3. (Fig. 2c). In the laboratory, resource depletion is a commonly used method to induce meiosis and sexual reproduction in some species, such as yeast. For our study, there was no significant change in expression of SPO11-2 and SPO11-3 in *P. tricornutum* cells following exposure to resource exhausted seawater. Some evidence has also been presented that shows ammonium induction may help regulate sexual reproduction in several diatom species, suggesting that it could serve as a key environmental factor regulating the sexual cycle across centric diatoms (Moore et al., 2017). However, our results showed that addition of ammonium to the media decreased mRNA expression of both SPO11 homologues. The two genes had different expression patterns, implying that they play specific functions in different biological processes. We speculate that the function of PtSPO11-3 is related to mitosis, while the function of PtSPO11-2 is related to meiosis. Due to its small cellular size and complex morphological changes, the meiosis and sexual reproduction process of *P. tricornutum* have not been directly observed, but our results provide clues in detecting the possible sexual cycle in this model organism. The low temperature, in which high expression of PtSPO11-2 was induced, may be a noteworthy factor to induce *P. tricornutum* to enter the sexual reproductive mode.

3.3. PtSPO11-3 rather than PtSPO11-2 works as an oligomer and interacts with Topo VI B

SPO11 is homologous to the catalytic subunit of the DNA topoisomerase VI (Topo VI A) (Bergerat et al., 1997). Topo VI is a heterotetramer composed of two A and two B subunits and is required for the progression of endoreduplication cycles (Kirik et al., 2007). The two Topo VI A subunits directly interact with each other. The A subunit dimer of TopoVI is assembled in a head to tail configuration in which the catalytic tyrosine within the WHD of one monomer is close to the Toprim domain of the other, creating the catalytic core of the enzyme. Similar to the model proposed for TopoVIA, SPO11 is believed to also act as a dimer, interacting in a head to tail pattern to introduce two coordinated active sites (Liu et al., 1995; Robert et al., 2016b; Vrielynck et al., 2016). However, the self-interactions of SPO11 may require additional proteins specific for meiotic cells, such as REC102, 104, 114, or SKI8 found in *S. cerevisiae* (Li et al., 2006; Maleki et al., 2007; Sasanuma et al., 2007). This protein complex could be regulated by posttranslational modifications (Hartung et al., 2007) and might only present during the onset of meiosis. Therefore, self-interaction might be an important clue for homologues to Topo VI A or SPO11. To determine which copy of the homologue of SPO11 is the orthologue, we tested which variant could self-interact in a yeast two-hybrid screen. We found that when PtSPO11-3 was fused to the GAL4 DNA-binding domain and GAL4 activation domain, host cells could grow very well on medium lacking histidine, suggesting a strong interaction of the test protein (Fig. 3). This same self-interaction was not detected when a PtSPO11-2 fusion was used. Furthermore, the reporter gene (HIS3) was not activated when SPO11-3 was fused to the GAL4 DNA-binding domain, PtSPO11-2 was fused to the GAL4 activation domain, or vice versa (Fig. 3). Additionally, the interaction between PtSPO11-3/2 and Topo VI B was also analyzed using a yeast two hybrid system. PJ69-4A was co-transformed with PtSPO11-3 fused with the GAL4 activation domain

and TopoVIB fused with the GAL4 DNA-binding domain. Plaques were observed 6 days after inoculating host cells in medium lacking histidine, suggesting interactions of PtSPO11-3 and Topo VI B (Fig. 3). Contrarily, interactions between PtSPO11-2 and Topo VI B were not detected. Consistent with the results from the phylogenetic analyses, these results suggest that SPO11-3 but not SPO11-2 might be a TopoVIA subunit in *P. tricornutum*.

3.4. Complementary approaches and functional assessment

The function of meiosis-specific genes inferred by bioinformatic analyses in the sexual reproduction of different organisms remains ambiguous without direct functional analysis (Schurko et al., 2009). Thus, the direct functional analysis of speculated meiosis-specific genes was necessary.

Although *P. tricornutum* is genetically transformable (Siaut et al., 2007; De Riso et al., 2009; Trentacoste et al., 2013), and gene knockout procedure has been established (Nymark et al., 2016; Serif et al., 2018; Slattery et al., 2018), however, because the meiosis process has never been observed in *P. tricornutum* before and the phenotypic changes are also undiscernible, it is unrealistic to analyze the function of meiosis-related genes directly in *P. tricornutum*. Budding yeast provides a powerful genetic system for elucidating the function of meiotic-related genes found in marine pennate diatoms. The system allows deletion of any chromosomal gene by homologous recombination and episomal expression of a mutant allele in the same cell (Hunt and Hassold, 2002).

As a complementary approach and functional assessment of candidate genes in *P. tricornutum* that were identified by bioinformatic analyses, the homozygous diploid strain of a *SPO11*-deleted mutant (BY4743, *spo*11Δ) was transformed individually with the two pYC2/NTC plasmids containing *SPO11* homologs (*SPO11-2* and *SPO11-3*). Analysis with the stable transformants were performed to characterize the kinetics and efficiency of spore production and compared with *spo*11Δ mutant and wild type (WT) yeast cells. Yeast cells were added to sporulation media, and aliquots were collected at different time intervals. The percentage of mature ascus containing 2, 3, or 4 spores was calculated after the cells were stained with DAPI. As shown in Fig. 4a, 2.5 days after the cells were transferred to the sporulation medium, the greatest number of bi-, tri- and/or tetranucleate cells were produced in wild type yeast strain, with numbers dropping during the liberation of spores after the rupture of the sporangium wall. The sporulation efficiency of the S288C background wild type strain was 31.4 ± 5.6%. Microscopic inspection indicated that tetranucleate cells were also present in *spo*11Δ mutant cells. However, the sporulation efficiency in *spo*11Δ (6.9 ± 3.6%) was far below that in the WT strain (Fig. 4a). Thus, deletion of the *SPO11* gene markedly decreased the sporulation efficiency by approximately 80%. Introduction of the *PtSPO11-3* gene did not significantly improved the sporulation efficiencies of the *spo*11Δ strain. Nevertheless, the *SPO11-2* strain showed a significant elevation in sporulation efficiency compared with the *spo*11Δ strain. Similar to WT, the percentage of cells with 2, 3 or 4 nuclei in the *SPO11-2* strain maximized at 26.6 ± 3.3%. The complementary analysis results herein suggest that the *PtSPO11-2* gene (chr_10:681001–682299) is a *bona fide* orthologue of *SPO11* in *P. tricornutum*. Representative images of wild type, SPO11 mutant and two other strains that had been incubated in sporulation media for 2.5 days are shown in Fig. 4b.

The conserved catalytic tyrosine in the WHD of SPO11 is essential for DSBs formation in several species (Bergerat et al., 1997; Hartung et al., 2007; Carofiglio et al., 2013; Robert et al., 2016a). The domain triggers the nucleophilic attack on the phosphodiester DNA back-bone, thus generating a transient covalent phosphodiester link between the catalytic tyrosine and the 5′end of the DNA break, allowing the invasion of allelic DNA strands and final processing of the recombination (Liu et al., 1995; Keeney and Neale, 2006). We noticed that a single tyrosine residue (tyrosine 140) in *P. tricornutum* existed at the same position in all the homologues in our alignment (Fig. 1a), which corresponded to the inferred catalytic site of SPO11 homologues. To further investigate this finding, we generated mutants of *PtSPO11-2* (*SPO11-2 M*), in which the TAC codon for the presumed catalytic residue tyrosine 140 was substituted by a TTC codon (F, phenylalanine), by using a site-directed mutagenesis method (Fig. 5a). Next, we transformed yeast cells carrying a homozygous disruption of *SPO11* with *PtSPO11-2 M* containing pYC2/NTC vectors. The transformation had no apparent effect on the progression of mitotic division cycles and proliferation; however, the sporulation efficiency of the *PtSPO11-2 M* transformed yeast strain was significantly lower than the *SPO11-2* strain (Fig. 5b). In other words, site-specific mutagenesis of the presumed catalytic residue tyrosine 140 in *P. tricornutum SPO11-2* abolished its ability to rescue the corresponding mutant of *S. cerevisiae*. These results show that tyrosine 140 of *P. tricornutum SPO11-2* is important to its activity and supports our sequence alignment and complementary results, suggesting a conserved mechanism for its meiotic functions.

A number of well-studied eukaryotes, including several parasitic protists, are thought to lack a meiotic process but nevertheless possess meiosis-specific gene orthologues in their genomes (Ramesh et al., 2005). It is clearly risky to rely only on analyzing the presence and absence of representative meiotic genes using phylogenetic studies to proclaim that an organism is sexual or asexual. Once meiosis is lost, meiotic specific genes are freed from selective constraints. They may accumulate mutations and gradually lose their meiotic-related functions, eventually becoming pseudogenes, non-sense DNA or new genes (Lynch and Conery, 2000; Forche et al., 2008; Hall and Colegrave, 2008). Therefore, verifying the meiotic function of putative meiotic genes in meiosis provides stronger inferences about meiosis and sexual reproduction than simply determining genes' presence or absence in genome. *SPO11* is an important part of the 'meiotic inventory' that has been used to indicate whether lineages are likely to be capable of sex (Ramesh et al., 2005; Malik et al., 2008; Bloomfield, 2016). Results herein indicate that one of the *P. tricornutum* SPO11 homologs, *PtSPO11-2*, matches its meiotic function and could rescue the corresponding mutant of *S. cerevisiae*. Thus, although meiosis has not been observed directly, the presence of a functional meiosis-specific SPO11 gene is a positive clue that meiosis and sexual reproduction could exist in this diatom. A more thorough comprehensive understanding of the functions of other representative meiotic-specific genes and their interacting proteins will ultimately provide important insights into the reproduction of this alga.

P. tricornutum is a coastal species with limited dispersal potential and is absence in the open ocean (Malviya et al., 2016). Clonal population structure, fixed heterozygosity and deviation from HWE have been used as evidence for *P. tricornutum* being classified as an asexual species (Falciatore et al., 1999; De Riso et al., 2009). However, whole genome sequencing of the 10 most studied strains, Pt0 – Pt10, (De Martino et al., 2007; Abida et al., 2015; Bailleul et al., 2015) have been performed recently and results indicate that Pt4 possesses the least number of heterozygous variant alleles, most of which follow HWE (Rastogi et al., 2020). It is interesting to note that Pt4 was collected from high latitudes where seasonal changes in seawater temperature are dramatic. Our results that suggest meiosis-specific gene is induced in *P. tricornutum* at low temperature conditions seem to resemble the natural niche of Pt4 (Bailleul et al., 2010). Therefore, sampling species across a more broad geospatial scale would be an interesting and informative strategy to explore the comprehensive landscape of the genomic diversity of this marine diatom.

4. Conclusions

P. tricornutum is a marine pennate diatom that is widely used to study diatom physiology and ecology for decades. Since the meiotic process and sexual cycle have never been observed directly, *P. tricornutum* has been considered to be an asexual species. Two copies of differently transcribed SPO11 homologs that contain the conserved

motifs of Winged-helix and Toprim domains were identified in *P. tricornutum*. The homolog PtSPO11-3 interacts with TopoVIB in yeast two-hybrid analysis, whereas the homolog PtSPO11-2 matches its meiotic function and could rescue the sporulation defect of a Spo11 yeast mutant strain. PtSPO11-2 was also found to be significantly up-regulated at low temperatures in *P. tricornutum* and its key catalytic residue was important to the homolog's function in sporulation. The occurrence of one factor of miosis cannot be a proof to ensure the entire process, but SPO11 is, in general, one of the critical components of miosis and the conservation of their important residues, structures, and meiotic function within yeast cells are positive signs of meiosis and sexual reproduction in this diatom.

CRediT authorship contribution statement

Yufeng Mao: Methodology, Investigation, Data curation, Visualization, Formal analysis, Writing - original draft. **Li Guo:** Data curation, Project administration. **Yan Luo:** Formal analysis, Data curation. **Zhihong Tang:** Investigation. **Wi Li:** Methodology, Formal analysis, Validation, Writing - review & editing. **Wen Dong:** Methodology, Investigation, Data curation, Visualization, Formal analysis, Supervision, Writing - original draft, Writing - review & editing.

Declaration of Competing Interest

The authors declare that they have no known competing financial interests or personal relationships that could have appeared to influence the work reported in this paper.

Funding and acknowledgments

This work was supported by the National High Technology Research and Development Program of China (2014AA022001), Earmarked Fund for Modern Agro-industry Technology Research System (YB201712051322) and Shandong Provincial Natural Science Foundation, China (ZR2011CQ047).

References

Abida, H., Dolch, L.J., Mei, C., Villanova, V., Conte, M., Block, M.A., et al., 2015. Membrane glycerolipid remodeling triggered by nitrogen and phosphorus starvation in *Phaeodactylum tricornutum*. Plant Physiol. 167, 118–136.

Bailleul, B., Berne, N., Murik, O., Petroutsos, D., Prihoda, J., Tanaka, A., et al., 2015. Energetic coupling between plastids and mitochondria drives CO_2 assimilation in diatoms. Nature 524, 366–369.

Bailleul, B., Rogato, A., De Martino, A., Coesel, S., Cardol, P., Bowler, C., et al., 2010. An atypical member of the light-harvesting complex stress-related protein family modulates diatom responses to light. Proc. Natl. Acad. Sci. U.S.A. 107, 18214–18219.

Bergerat, A., De Massy, B., Gadelle, D., Varoutas, P.C., Nicolas, A., Forterre, P., 1997. An atypical topoisomerase ii from archaea with implications for meiotic recombination. Nature 386, 414–417.

Biasini, M., Bienert, S., Waterhouse, A., Arnold, K., Studer, G., Schmidt, T., et al., 2014. Swiss-model: modelling protein tertiary and quaternary structure using evolutionary information. Nucl. Acids Res. 42, W252–W258.

Bloomfield, G., 2016. Atypical ploidy cycles, Spo11, and the evolution of meiosis. Semin. Cell Dev. Boil. 54, 158–164.

Bowler, C., Allen, A.E., Badger, J.H., Grimwood, J., Jabbari, K., et al., 2008. The *Phaeodactylum* genome reveals the evolutionary history of diatom genomes. Nature 456, 239–244.

Brachmann, C.B., Davies, A., Cost, G.J., Caputo, E., Li, J., et al., 1998. Designer deletion strains derived from *Saccharomyces cerevisiae* S288C: a useful set of strains and plasmids for PCR-mediated gene disruption and other applications. Yeast 14, 115–132.

Bulankova, P., Riehs-Kearnan, N., Nowack, M.K., Schnittger, A., Riha, K., 2010. Meiotic progression in *Arabidopsis* is governed by complex regulatory interactions between SMG7, TDM1, and the meiosis I–specific cyclin TAM. Plant Cell. 22, 3791–3803.

Carofiglio, F., Inagaki, A., Vries, S.D., Wassenaar, E., Schoenmakers, S., Vermeulen, C., et al., 2013. Spo11-independent DNA repair foci and their role in meiotic silencing. Plos Genet. 9, e1003538.

Chen, S.J., Wang, J.C., 1998. Identification of active site residues in *Escherichia coli* DNA topoisomerase I. J. Biol. Chem. 273, 6050–6056.

Chepurnov, V.A., Mann, D.G., Von, D.P., Vanormelingen, P., Gillard, J., Inzé, D., et al., 2010. In search of new tractable diatoms for experimental biology. BioEssays 30, 692–702.

Chiu, J., March, P.E., Lee, R., Tillett, D., 2004. Site-directed, Ligase-Independent Mutagenesis (SLIM): a single-tube methodology approaching 100% efficiency in 4 h. Nucl. Acids Res. 32, e174.

Crismani, W., Girard, C., Mercier, R., 2013. Tinkering with meiosis. J. Exp. Bot. 64, 55–65.

Dacks, J.B., Doolittle, W.F., 2001. Reconstructing/decon-structing the earliest eukaryotes: how comparative genomics can help. Cell 107, 419–425.

De Martino, A.M., Juan Shi, A., Bowler, K.P., 2007. Genetic and phenotypic characterization of *Phaeodactylum tricornutum* (*Bacillariophyceae*) accessions. J. Phycol. 43, 992–1009.

De Riso, V., Raniello, R., Maumus, F., Rogato, A., Bowler, C., Falciatore, A., 2009. Gene silencing in the marine diatom *Phaeodactylum tricornutum*. Nucl. Acids Res. 37, e96.

Edgar, R., 2004. MUSCLE: multiple sequence alignment with high accuracy and high throughput. Nucl. Acids Res. 32, 1792–1797.

Falciatore, A., Casotti, R., Leblanc, C., Abrescia, C., Bowler, C., 1999. Transformation of nonselectable reporter genes in marine diatoms. Mar. Biotechnol. 1, 239–251.

Forche, A., Alby, K., Schaefer, D., Johnson, A.D., Berman, J., Bennett, R.J., 2008. The parasexual cycle in *Candida albicans* provides an alternative pathway to meiosis for the formation of recombinant strains. PLoS Biol. 6, e110.

Gietz, R.D., Schiestl, R.H., 2007. High-efficiency yeast transformation using the LiAc/SS carrier DNA/PEG method. Nat. Protoc. 2, 38–41.

Guillard, R.R.L., 1975. Culture of phytoplankton for feeding marine invertebrates. culture of marine invertebrate animals, Springer US, pp. 29-60.

Hall, A.R., Colegrave, N., 2008. Decay of unused characters by selection and drift. J. Evol. Biol. 21, 610–617.

Hartung, F., Angelis, K.J., Meister, A., Schubert, I., Melzer, M., Puchta, H., 2002. An archaebacterial topoisomerase homolog not present in other eukaryotes is indispensable for cell proliferation of plants. Curr. Biol. 12, 1787–1791.

Hartung, F., Puchta, H., 2001. Molecular characterization of homologues of both subunits A (SPO11) and B of the archaebacterial topoisomerase 6 in plants. Gene. 271, 81–86.

Hartung, F., Wurz-Wildersinn, R., Fuchs, J., Schubert, I., Suer, S., Puchta, H., 2007. The catalytically active tyrosine residues of both spo11-1 and spo11-2 are required for meiotic double-strand break induction in arabidopsis. Plant Cell 19, 3090–3099.

Hunt, P.A., Hassold, T.J., 2002. Sex matters in meiosis. Science 296, 2181–2183.

Jain, M., Tyagi, A.K., Khurana, J.P., 2008. Constitutive expression of a meiotic recombination protein gene homolog, OsTOP6A1, from rice confers abiotic stress tolerance in transgenic Arabidopsis plants. Plant Cell Rep. 27, 767–778.

Kee, K., Protacio, R.U., Arora, C., Keeney, S., 2004. Spatial organization and dynamics of the association of rec102 and rec104 with meiotic chromosomes. EMBO J. 23, 1815–1824.

Keeney, S., Neale, M.J., 2006. Initiation of meiotic recombination by formation of DNA double-strand breaks: mechanism and regulation. Biochem. Soc. Trans. 34, 523–525.

Kirik, V., Schrader, A., Uhrig, J.F., Hulskamp, M., 2007. MIDGET unravels functions of the *Arabidopsis* topoisomerase VI complex in DNA endoreduplication, chromatin condensation, and transcriptional silencing. Plant Cell. 19, 3100–3110.

Li, J., Hooker, G.W., Roeder, G.S., 2006. *Saccharomyces cerevisiae* Mer2, Mei4 and Rec114 form a complex required for meiotic double-strand break formation. Genetics 173, 1969–1981.

Liu, J., Wu, T.C., Lichten, M., 1995. The location and structure of double-strand DNA breaks induced during yeast meiosis: evidence for a covalently linked DNA-protein intermediate. EMBO J. 14, 4599–4608.

Livak, K.J., Schmittgen, T.D., 2001. Analysis of relative gene expression data using real-time quantitative PCR and the $2^{-\Delta\Delta CT}$ method. Methods 25, 402–408.

Lynch, M., Conery, J.S., 2000. The evolutionary fate and consequences of duplicate genes. Science. 290, 1151–1155.

Maheswari, U., Jabbari, K., Petit, J.L., Porcel, B.M., Allen, A.E., et al., 2010. Digital expression profiling of novel diatom transcripts provides insight into their biological functions. Genome Biol. 11, R85.

Maleki, S., Neale, M.J., Arora, C., Henderson, K.A., Keeney, S., 2007. Interactions between Mei4, Rec114, and other proteins required for meiotic DNA double-strand break formation in *Saccharomyces cerevisiae*. Chromosoma 116, 471–786.

Malik, S.B., Pightling, A.W., Stefaniak, L.M., Schurko, A.M., Logsdon Jr, J.M., 2008. An expanded inventory of conserved meiotic genes provides evidence for sex in *Trichomonas vaginalis*. PloS One 3, e2879.

Malik, S.B., Ramesh, M.A., Hulstrand, A.M., Logsdon, J.M., 2007. Protist homologs of the meiotic Spo11 gene and topoisomerase VI reveal an evolutionary history of gene duplication and lineage-specific loss. Mol. Biol. Evol. 24, 2827–2841.

Malviya, S., Scalco, E., Audic, S., Vincent, F., Veluchamy, A., Poulain, J., et al., 2016. Insights into global diatom distribution and diversity in the world's ocean. Proc. Natl. Acad. Sci. U.S.A. 113, E1516–E1525.

Marchler-Bauer, A., Derbyshire, M.K., Gonzales, N.R., Lu, S., Chitsaz, F., Geer, L.Y., et al., 2015. Cdd: ncb's conserved domain database. Nucleic Acids Res. 43, 222–226.

Moore, E.R., Bullington, B.S., Weisberg, A.J., Jiang, Y., Chang, J., Halsey, K.H., 2017. Morphological and transcriptomic evidence for ammonium induction of sexual reproduction in *Thalassiosira pseudonana* and other centric diatoms. PloS One 12 (7), e0181098.

Nymark, M., Sharma, A.K., Sparstad, T., Bones, A.M., Winge, P., 2016. A CRISPR/Cas9 system adapted for gene editing in marine algae. Sci. Rep. 6, 24951.

Patil, S., Moeys, S., Von Dassow, P., Huysman, M.J., Mapleson, D., De Veylder, L., et al., 2015. Identification of the meiotic toolkit in diatoms and exploration of meiosis-specific SPO11 and RAD51 homologs in the sexual species *Pseudo-nitzschia multistriata* and *Seminavis robusta*. BMC Genom. 16, 930.

Ramesh, M.A., Malik, S.B., Logsdon, J.M., 2005. A phylogenomic inventory of meiotic genes: evidence for sex in *Giardia* and an early eukaryotic origin of meiosis. Curr. Biol. 15, 185–191.

Rastogi, A., Vieira, F.R.J., Cabanilas, A.F.D., Veluchamy, A., Cantrel, C., Wang, G., et al., 2020. A genomics approach reveals the global genetic polymorphism, structure, and functional diversity of ten accessions of the marine model diatom *Phaeodactylum tricornutum*. ISME J. 14, 347–363.

Robert, T., Nore, A., Brun, C., Maffre, C., Crimi, B., Bourbon, H.M., et al., 2016a. The topovib-like protein family is required for meiotic DNA double-strand break formation. Science 351, 943–949.

Robert, T., Vrielynck, N., Mézard, C., de Massy, B., Grelon, M.A., 2016b. new light on the meiotic DSB catalytic complex. Semin. Cell Dev. Boil. 54, 165–176.

Sasanuma, H., Murakami, H., Fukuda, T., Shibata, T., Nicolas, A., Ohta, K., 2007. Meiotic association between spo11 regulated by rec102, rec104 and rec114. Nucl. Acids Res. 35, 1119–1133.

Schurko, A.M., Neiman Jr., M., 2009. Signs of sex: what we know and how we know it. Trends Ecol. Evol. 24, 208–217.

Serif, M., Dubois, G., Finoux, A.L., Teste, M.A., Jallet, D., Daboussi, F., 2018. One-step generation of multiple gene knock-outs in the diatom *Phaeodactylum tricornutum* by DNA-free genome editing. Nat. Commun. 9, 3924.

Siaut, M., Heijde, M., Mangogna, M., Montsant, A., Coesel, S., Allen, A., et al., 2007. Molecular toolbox for studying diatom biology in *Phaeodactylum tricornutum*. Gene 406, 23–35.

Slattery, S.S., Diamond, A., Wang, H., Therrien, J.A., Lant, J.T., Jazey, T., et al., 2018. An expanded plasmid-based genetic toolbox enables Cas9 genome editing and stable maintenance of synthetic pathways in *Phaeodactylum tricornutum*. ACS Synth. Biol. 7, 328–338.

Sprink, T., Hartung, F., 2014. The splicing fate of plant SPO11 genes. Front Plant Sci. 5, e00214.

Stacey, N.J., Kuromori, T., Azumi, Y., Roberts, G., Breuer, C., Wada, T., et al., 2006. *Arabidopsis* spo11-2 functions with spo11-1 in meiotic recombination. Plant J. 48, 206–216.

Trentacoste, E.M., Shrestha, R.P., Smith, S.R., Glé, C., Hartmann, A.C., Hildebrand, M., et al., 2013. Metabolic engineering of lipid catabolism increases microalgal lipid accumulation without compromising growth. Proc. Natl. Acad. Sci. USA 110, 19748–19753.

Villeneuve, A.M., Hillers, K.J., 2001. Whence meiosis? Cell 106, 647–650.

Von Dassow, P., Montresor, M., 2011. Unveiling the mysteries of phytoplankton life cycles: patterns and opportunities behind complexity. J. Plankton Res. 33, 3–12.

Vrielynck, N., Chambon, A., Vezon, D., Pereira, L., Chelysheva, L., De Muyt, A., et al., 2016. A DNA topoisomerase VI–like complex initiates meiotic recombination. Science 351, 939–943.

Wach, A., Brachat, A., Pohlmann, R., Philippsen, P., 1994. New heterologous modules for classical or PCR-based gene disruptions in *Saccharomyces cerevisiae*. Yeast 10, 1793–1808.

Wendorff, T.J., Berger, J.M., 2018. Topoisomerase VI senses and exploits both DNA crossings and bends to facilitate strand passage. ELife 7, e31724.

Yin, Y., Cheong, H., Friedrichsen, D., Zhao, Y., Hu, J., Mora-Garcia, S., Chory, J., 2002. A crucial role for the putative Arabidopsis topoisomerase VI in plant growth and development. PNAS 99, 10191–10196.